PERGAMON

Computers in Biology and Medicine 30 (2000) 71–88

Computers in Biology and Medicine

www.elsevier.com/locate/compbiomed

Self-organizing arterial pressure pulse classification using neural networks: theoretical considerations and clinical applicability

Chuang-Chien Chiu[a,*], Shoou-Jeng Yeh[b], Ching-Hsiu Chen[a]

[a] *Department of Automatic Control Engineering, Feng Chia University, Taichung, Taiwan, ROC*
[b] *Section of Neurology and Neurophysiology, Cheng-Ching General Hospital, Taiwan, ROC*

Received 3 June 1999; accepted 2 November 1999

Abstract

A self-organizing classification system for the arterial pressure pulse based on the ART2 (adaptive resonance theory) network was developed. The system consists of a preprocessor and an ART2 recognition network. The preprocessor removes the arterial pressure pulse servo component signals from Finapres, detects the systolic pressure points and divides the acquired signals into minimal cardiac cycles. The ART2 network input is the minimal cardiac cycle detected by the preprocessor. The classification results can be used to assist physicians in evaluating the signs of abnormal and normal autonomic control and has shown its clinical applicability for the examination of the autonomic nervous system.

Keywords: Self-organizing; ART2 network; Finapres; Minimal cardiac cycles; Autonomic nervous system

1. Introduction

Focusing on the research studies of autonomic nervous system (ANS) [1], we know that most standard laboratory tests of cardiovascular autonomic function rely on the measurement of heart rate (HR) variability and blood pressure (BP), which are used as the indices of evaluating the sympathetic and parasympathetic cardiomotor activities. However, the

* Corresponding author. Tel.: +886-4-451-7250; fax: +886-4-451-9951.
E-mail address: chiuc@auto.fcu.edu.tw (C.-C. Chiu).

0010-4825/00/$ - see front matter
PII: S0010-4825(99)00023-2

traditional clinical methods for assessing neural control of the circulation monitoring both HR and BP have some defects. First, in order to acquire valid HR and BP, most measurements must be obtained separately. This process is very costly and sometimes invasive. Second, short-term signal acquisition and analysis, which provides insufficient information for clinicians, is widely adopted in the laboratory evaluation of autonomic reflex function. Third, most measurement instruments have unsatisfactory sensitivity. These defects reduce the efficiency of clinicians in diagnosing patients and therefore delay the treatment. Accordingly [2], the ideal mode of measurement should be noninvasive, applicable over a wide range of conditions, reproducible, easy to implement and require an acceptable learning curve. Moreover, the data acquisition should be continuous, hands off and bad data should be automatically rejected. Last, the ideal method should be affordable. The finger arterial pressure (Finapres) device, by which the arterial pressure pulse, BP and HR are measured noninvasively in the finger, provides a beat-to-beat alternative for continuous recordings and long-term examination. The contour of the arterial pressure pulse generated by Finapres generally correlates well with intra-arterial measurements from the radial or brachial artery [3,4].

Many researchers have developed various methods to analyze beat-to-beat BP and HR variability in the past. The analysis of BP and HR variability in the frequency domain has been useful in pathophysiologic research into the nature of cardiovascular regulation. DeBoer et al. [5] presented two approaches: the so-called the interval spectrum and the spectrum of counts to analyze the HR variability. Karemaker [6] used the interval spectrum to estimate the spectrum of BP variability. Saul et al. [7] presented the transfer-function analysis for BP and HR variability. However, there is still inadequate research into the sensitivity and specificity of the analysis of cardiovascular variability based on noninvasive continuous recording of the arterial pressure pulse. Chiu et al. [8] presented methods for correctly acquiring the signals from a Finapres device. The Chiu method allows simultaneous recording, storage and analyzing of the acquired signals. From the results of the preliminary analysis, Chiu et al. found that the power spectra of pulse signals with servo components removed had more preferable results than those from the original signals. Also, the continuously acquired pulse signals could be used to derive physiological data the same as that from the RS232 Finapres port (providing discrete HR and BP data). This fact convinced us that one could analyze the Finapres signals using continuously acquired pulse signals instead of signals from the RS232 port. Chiu et al. also demonstrated that continuous recording of beat-to-beat arterial pressure pulse signals could afford valuable information to understand central autonomic regulation [9]. Let us first review the physiological functions of the pulse waveform in the time domain. As the scheme shown in Fig. 1, there are many characteristic parameters to indicate the different physiological states, such as A wave, P (percussion) wave, T (tidal) wave, D (dichotic) wave, U (up stroke) point, V notch (i.e. Dichotic notch) and the height of *Dh*, etc. The corresponding physiological state for each segment is as follows. The segment between Q and U represents the pulse transmission time. The segment between V and D represents the diastolic shut time. The segment of U and P represents the systolic ejection time. The segment between U and U′ represents one cardiac cycle. The segment between P and V represents the ejection slow time.

Therefore, the *shape* of the pulse waveform provides important information to doctors for diagnosis. In the traditional methods, the doctor diagnosed the shape and position of every parameter of the pulse using their own judgements. Recently, many mathematical methods

have been presented to assist doctors in judging the shape of a pulse, such as the slope method. However, these methods are not easy to use. It is difficult to judge different kinds of pulses using a fixed threshold. It is desirable for a recognition system to adjust its threshold in association with the changes in the environment. In this study, we adopted an adaptive resonance theory neural network (ART2) [10] recognition system, implemented using the learning and self-organizing mechanisms of template patterns as in the decision-making processes of human beings. The ART2 can be used to categorize continuous pulse signals from a Finapres device.

The main focus of this study was to develop a self-organizing pulse-signal classification system for the arterial pressure pulse. Moreover, the classification results of the ART2 network, provides an alternative method for evaluating autonomic functions and were used to assist physicians in evaluating the beat-to-beat arterial pressure pulse for signs of abnormal and normal autonomic control. The system configuration is shown in Fig. 2. The ART2-based classification system includes a preprocessor and a recognition system. The continuous recording of arterial pressure pulse is obtained noninvasively, using the finger photoplethysmography technique, i.e. Finapres blood pressure monitor model 2300, Ohmeda. Finapres signals are sent to an external device through two ports: BP (including systolic pressure, diastolic pressure and mean pressure) and HR can be obtained from the RS232 output port and the arterial pressure pulse signal obtained from the analog output (AO) port. The input signal from the preprocessor is a continuously acquired signal from the Finapres analog output. The output results from the preprocessor are the minimal cardiac cycles. These cardiac cycles are the input for ART2 networks. ART2 categorizes these input patterns adaptively. The ART2 will be discussed in greater detail later in this paper.

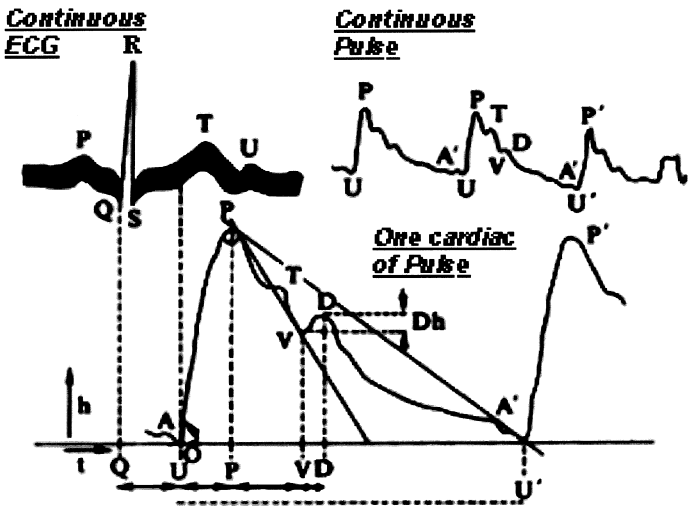

Fig. 1. The characteristic parameters of the ECG and pulse waveform.

2. Material and methods

2.1. Finapres

The Finapres device operation, which is fully automated, is described briefly as follows. As one knows, the ability to measure arterial pressure rapidly and noninvasively through the finger involves the principle of arterial wall unloading. The blood volume under an inflatable finger cuff is measured with an infrared plethysmograph and kept to a constant set point value by controlling the cuff pressure in response to volume changes in the finger artery. By means of a built-in servo adjustment mechanism, a proper volume-clamped set point is established and adjusted at regular intervals. In other words, the high-speed servo system rapidly inflates and deflates the cuff to maintain the photoplethysmographic output constant at the unloaded state. However, this procedure interrupts the blood pressure recording (usually for 2–3 beats every 70 beats). Note that the regular servo adjustment is essential to keep the finger arteries fully unloaded and the transmural pressure equal to zero. At zero transmural pressure, the arterial finger pressure is equal to the cuff pressure. The modules, which cause the regular servo adjustment of the continuously acquired pulse signal, are called *servo components*. In our previous study [8], we used a personal computer combined with a general-purpose data acquisition board and LabVIEW environment to develop techniques for acquiring signals correctly from a Finapres monitor. These acquired signals can then be recorded, stored and analyzed simultaneously in real time.

2.2. Preprocessor

The continuous pulse signals are first sent through a preprocessor before going to the ART2 for arterial pressure pulse classification. The key functions of the preprocessor are to remove the servo components from the continuous recording of arterial pressure pulse signals from

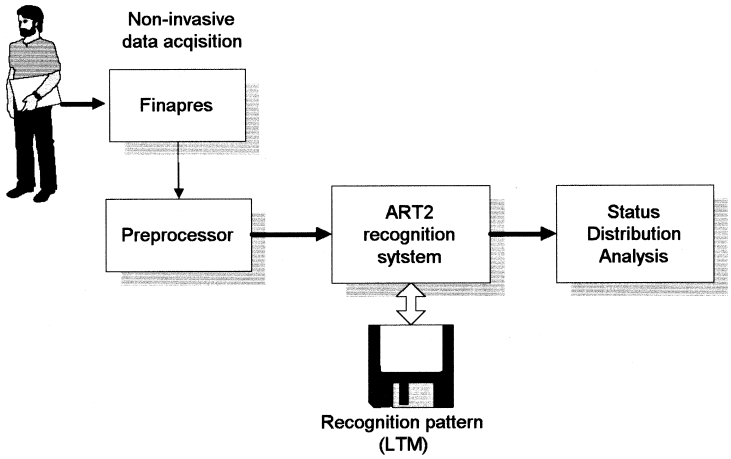

Fig. 2. System configuration.

Finapres and to divide the acquired signals into minimal cardiac cycles. As one knows, the length of each beat-to-beat cardiac cycle can be fluctuated. However, the input patterns in the ART2 input layer network must be of equal length. Therefore, the reason the acquired signals are divided into minimal cardiac cycles is to create the equal length input patterns for the ART2 network. The procedures of the preprocessor are listed below with an example to illustrate the extracted minimal cardiac cycle as shown in Fig. 3.

2.2.1. Initialization

Let $x(k)$ be the pulse signal acquired from the Finapres AO port. The maximum value within the very first 3 s duration input pulse signal is acquired. The sampling rate to acquire the Finapres signal was set at 60 Hz in this research. Thus, the time index for the first wave-peak (i.e. the systolic blood pressure), P_1, can be found as follows:

$$P_1 = \arg\max[x(k)], \quad 1 \le k \le 180$$

Note that $\arg\max[x(k)]$ represents the argument of function $x(k)$ in which the maximum value occurred. The mean, m and standard deviation, sd, of the HR periods (in seconds) from the original HR data provided by the Finapres RS232 port are calculated. Let I_P be the ceiling of $(m - sd) \times 60$ and I_V be the ceiling of $(m + 3sd) \times 60$. After P_1, the time index for the first wave valley (i.e. the diastolic blood pressure), V_1, can then be obtained using:

$$V_1 = \arg\min[x(k)], \quad P_1 \le k \le P_1 + I_V$$

Similarly, $\arg\min[x(k)]$ is the argument of function $x(k)$ in which the minimum value occurs.

2.2.2. Searching wave peaks and valleys

After P_1 and V_1 are found, the remaining of P_i's and V_i's can be derived recursively using the following formulas:

$$P_i = \arg\max[x(k)], \quad V_{i-1} \le k \le V_{i-1} + I_P$$

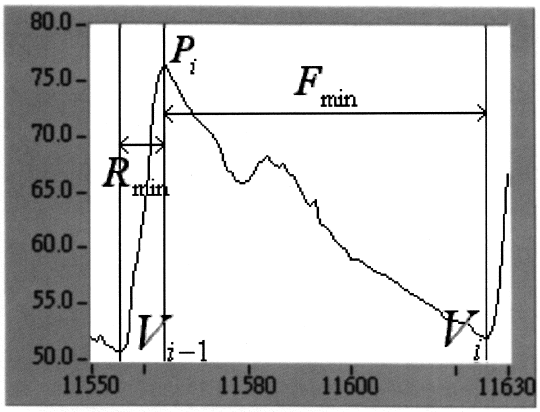

Fig. 3. An example to illustrate the extracted minimal cardiac cycle.

$$V_i = \arg\min[x(k)], \quad P_i \le k \le P_i + I_V$$

2.2.3. Removing the servo components

Two parameters are defined below for removing the servo components:

$$D_{rk} = x(P_k) - x(V_k)$$

and

$$D_{lk} = x(P_{k+1}) - x(V_k).$$

If either D_{rk} or D_{lk} is less than 25 mm Hg, then the entire duration from the time index P_k to V_{k+1} is treated as the dynamic servo segment and therefore, should be removed from the original AO signal.

2.2.4. Extracting the minimal cardiac cycles

Two parameters are defined below for extracting the minimal cardiac cycles. R_{min} is the minimal duration for the U–P segment (Fig. 1) in all input cardiac cycles. F_{min} is the minimal duration for the P–U′ segment (Fig. 1) in all input cardiac cycles. The length of the desired minimal cardic cycle is $(R_{min} + F_{min})$ seconds. The portion of each minimal cardiac cycle is truncated from each P_i point to the front R_{min} in length and to the rear F_{min} in length. Note that the sampling rate to acquire the Finapres signal is 60 Hz.

$$R_{min} = \min_{\forall i} \{(P_i - V_{i-1})/60\}$$

$$F_{min} = \min_{\forall i} \{(V_i - P_i)/60\}$$

The truncated minimal cardiac cycles, which contain significant physiological information from the cardiac cycles, are the inputs to the ART2 network for recognition. An example to illustrate the extracted minimal cardiac cycle is shown in Fig. 3.

2.3. ART2 neural network

Computing with artificial neural networks (ANNs) is one of the fastest growing fields in the history of artificial intelligence (AI), largely because ANNs can be trained to identify nonlinear patterns between input and output values and can solve complex problems much faster than digital computers [11]. There have been a number of neural network industrial applications [12]. Some neural networks have learning and self-organizing abilities. Researchers have found one answer to these questions through the attempt to solve a basic design problem, called the stability-plasticity dilemma, faced by all intelligent systems capable of autonomously adapting in real time to unexpected changes in their world. A developing theory called adaptive resonance theory (ART) suggests a solution to this problem [10]. ART is a neural network that self-organizes stable recognition code patterns in real-time in response to arbitrary sequences of input patterns. In this study, a self-organizing neural network (ART2) was employed to

categorize the continuous pulse signals. Due to its wide range of applicability and its ability to learn complex and nonlinear relationships, ART2 was applied to classify the pulse signals. In addition, ART2 has made strong advances in continuous speech recognition and synthesis, pattern recognition, classification of noisy data, nonlinear feature detection and other fields. ART2 is capable of high-speed parallel signal processing in real time. When used in medical diagnosis, ART2 is not affected by factors such as human fatigue, emotional states and monotony. Therefore, ART2 is capable of rapid identification, analysis of conditions and diagnosis in real time.

ART networks encode new input patterns, in part, by changing the weights, or long-term memory (LTM) traces, of a bottom-up adaptive filter. A typical ART2 architecture is shown in Fig. 4. This filter is contained in pathways leading from a feature representation field (F1) to a category representation field (F2), whose nodes undergo cooperative, (sometimes called *competitive learning*) shared by many other adaptive pattern recognition and associative learning models. In an ART network, however, it is a second, top-down adaptive filter that leads to the crucial property of code self-stabilization. Such top-down adaptive signals play the role of learned expectations in an ART system. They enable the network to carry out attention priming, pattern-matching and self-adjusting parallel search. One of the key insights of the ART design is that the top-down attention and intentional, or expectation, mechanisms are necessary to self-stabilized learning in response to an arbitrary input environment.

In Fig. 4, the fields F1 and F2, as well as the bottom-up and top-down adaptive filters, are contained within ART's *attentional subsystem*. An auxiliary *orienting subsystem* becomes active

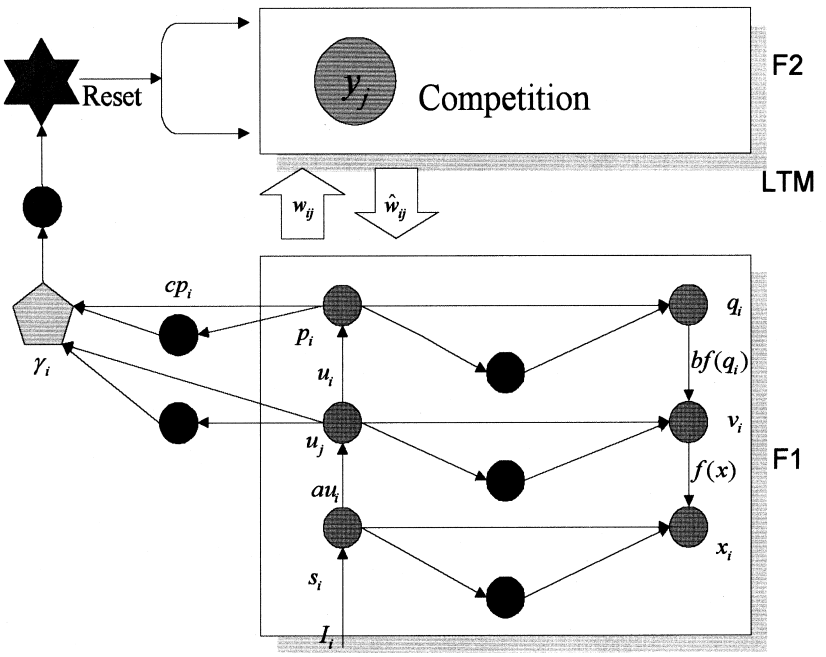

Fig. 4. A typical ART2 architecture.

when a bottom-up input to F1 fails to match the learned top-down expectation read-out by the active category representation at F2. In this case, the orienting subsystem is activated and causes a rapid reset of the active category representation at F2. This reset event automatically informs the attentional subsystem to proceed with a parallel search. Alternative categories are tested until either an adequate match is found or a new category is established. The search remains efficient because the search strategy is updated adaptively throughout the learning process. The search proceeds rapidly, relative to the *learning rate*. Thus, significant changes in the bottom-up and top-down adaptive filters occur only when a search ends and a matched F1 pattern resonates within the system. The bottom-up adaptive filtering, code or hypothesis selection, read-out of a top-down learned expectation, matching and code reset process cycle shows that, within an ART system, adaptive pattern recognition is a special case of the more general cognitive process of discovering, testing, searching, learning and recognizing hypotheses. The fact that learning within an ART system occurs only within a resonant state, enables such a system to solve the design tradeoff between plasticity and stability. Plasticity, or the potential for rapid change in the LTM traces, remains intact indefinitely, thereby enabling an ART architecture to learn about future unexpected events until it exhausts its full memory capacity.

Learning within a resonant state either refines the code of a previously established recognition code, based upon any new information that the input pattern may contain, or initiates code learning within a previously uncommitted set of nodes. For example, a new analog input pattern can be added at any time to the ART2. The system will then search the established categories. If an adequate match is found, possibly on the initial search cycle, the LTM category representation is refined, if necessary, to incorporate the new pattern. If no match is found and the full coding capacity is not yet exhausted, a new category is formed, with previously uncommitted LTM traces encoding the STM pattern established by the input. In an ART architecture, by contrast, a search takes place only as a recognition code is being learned and the search maintains its efficiency as learning goes on. Self-stabilization of prior learning is achieved via the dynamic buffering provided by a read-out of a learned top-down expectation, not by switching off plasticity or restricting the class of admissible inputs. In general, within the ART architecture, once learning self-stabilizes within a particular recognition category, the search mechanism is automatically disengaged. Thereafter, that category can be directly activated, or accessed, with great rapidity and without the need for a search by any of its input exemplars.

The criterion for an adequate match between an input pattern and a chosen category template is adjustable in the ART architecture. The matching criterion is determined by a vigilance parameter that controls activation of the orienting subsystem. All other things being equal, higher vigilance imposes a stricter matching criterion, which in turn partitions the input set into finer categories. Lower vigilance tolerates greater top-down/bottom-up mismatches at F1, leading in turn to coarser categories. In addition, at every vigilance level, the matching criterion is self-scaling: a small mismatch may be tolerated if the input pattern is complex, while the same feature mismatch would trigger a reset if the input is represented only by a few features. Note that the vigilance parameter ρ is set between 0 and 1. Detailed ART2 learning and self-organizing principles are described in the Appendix.

For simplicity, we henceforth consider an ART2 system in which F2 makes a choice and in

which e is set to be equal to 0. Thus, $\|x\| = \|u\| = \|q\| = 1$. The continuously differentiable signal function $f(\cdot)$ in the following equation is used for simulations. The ART2 parameters employed in the present system are shown in Table 1.

$$f(x) = \begin{cases} \dfrac{2qx^2}{x^2 + q^2}, & \text{if } 0 \le x < q \\ 0, & \text{if } x > q \end{cases}$$

3. Experimental results and discussion

In this study, the ART2 network was used to categorize continuous pulse signals from the Finapres device. In order to show the clinical applicability, two states of examination were undertaken. The supine state provides the baseline for the experiments. On the other hand, a 60° head-up tilt can be used to observe the autonomic control especially for the assessment of sympathetic activity. For each sample, a continuous pulse signal, containing both supine and 60° tilt states, was recorded. The total length of a pulse signal for each sample was 36,000 points (i.e. 10 min; sampling rate is 60 Hz) with each state containing approximately 18,000 points (i.e. the 5 min period). The acquired waveform was then sent to the preprocessor, presented in the previous section, to remove the servo components and extract the minimal cardiac cycles. The portion of each minimal cardiac cycle was then treated as a single input pattern for the ART2 network. These single patterns were sent to the ART2 network for categorization. Since the ART2 network is a self-organizing pattern recognition system, no training is needed for pattern recognition.

Two examples of ART2 recognition results, one for the normal case and one for the NIDDM (non-insulin-dependent diabetes mellitus) patient, are illustrated here to show the effectiveness of this method in evaluating the signs of abnormal and normal autonomic control. The acquired signal for the normal case, after removing the servo components, is shown in Fig. 5. The recognition templates (i.e. LTM) of ART2 for the normal case are shown in Fig. 6. There are five recognition categories. Applying the ART2 network to classify every minimal cardiac cycle, one can obtain the status distribution plot (SDP) as shown in Fig. 7. The SDP is helpful to determine the reasonable boundary related to different examination states in the

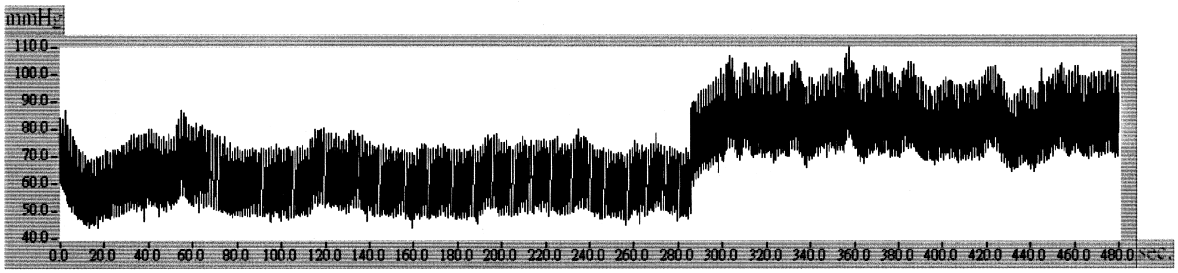

Fig. 5. An example of the acquired signal for the normal case from Finapres after removing the servo components.

Table 1
ART2 parameters employed in the present system

	a	b	c	d	θ	ε	ρ
Definition	feedback parameter in F1 layer	feedback parameter in F1 layer	parameter in orienting subsystem	activation level in F2 neuron	threshold	learning rate	vigilance parameter
Value	5	5	0.08	0.9	0.01	0.10	0.98

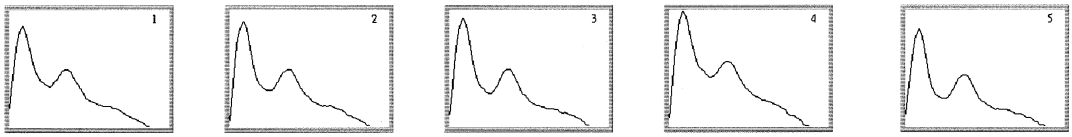

Fig. 6. The recognition categories of ART2 for the normal case shown in Fig. 5.

continuous waveform. It is clear that the changing index from supine to 60° incline is at the sequence number 244 in Fig. 7. We can observe that the reasonable changing index is at number 290 with the assistance of the ART2. Two spectra are shown in Fig. 8. The power spectral density (PSD) [13,14] of the continuously acquired arterial pressure pulse from Finapre for the normal case, with the removal of servo components, at the supine state is shown in Fig. 8(a). Also, the PSD of the continuously acquired arterial pressure pulse for the normal case, with the removal of servo components, at the 60° incline is shown in Fig. 8(b). Note that LF stands for the frequency range from 0.07 to 0.15 Hz, corresponding primarily to the sympathetic nerve activity. On the other hand, HF stands for the frequency range from 0.15 to 0.5 Hz corresponding primarily to the parasympathetic nerve activity [15]. For the normal case, the power spectra are increased in both the LF and HF areas when the states changed from the supine to the incline position.

The acquired signal for the NIDDM patient after removing the servo components is shown in Fig. 9. The recognition templates (i.e. LTM) of ART2 for this case are shown in Fig. 10. There are five recognition categories. Note that the matching criterion is determined by the vigilance parameter. For each sample, the same ART2 parameters are shown in Table 1 were applicable. The results in Fig. 10 are clearly different from those depicted in Fig. 6. These categories can be useful tools for diagnosis in clinical application. Applying the ART2 network to classify every minimal cardiac cycle, one can obtain a status distribution plot (SDP), as shown in Fig. 11. The changing index from supine to 60° incline is at the sequence number 525 (note that it is marked manually by the physician). However, for the signal of the NIDDM patient, it is somehow difficult for us to point out where the changing index is. In Fig. 12(a), the PSD of the continuously acquired arterial pressure pulse from Finapre for the NIDDM patient with the removal of servo components in the supine state is shown. Also, the PSD of the continuously acquired arterial pressure pulse with the removal of servo components in the

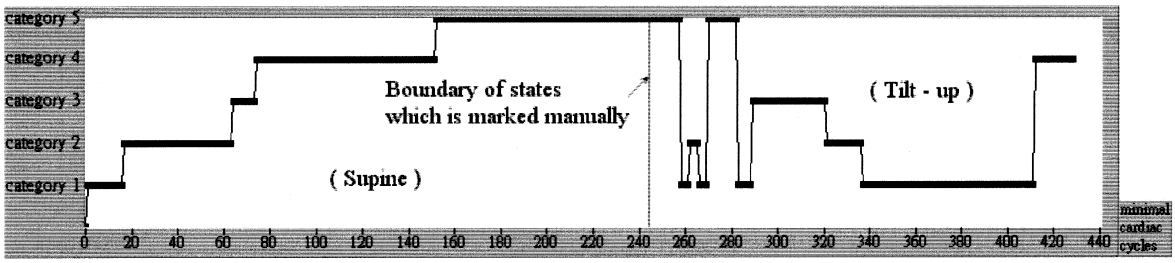

Fig. 7. Status distribution plot (SDP) for the normal case. Lateral axis is the continuous input numbers of minimal cardiac cycles. Straight axis: Category 1–5 denote five classified patterns.

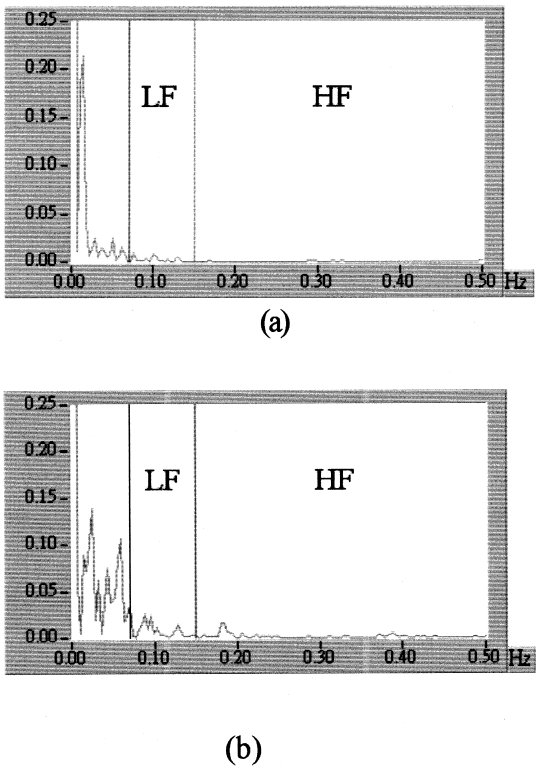

Fig. 8. (a) The power spectral density (PSD) of the continuously acquired arterial pressure pulses from Finapre for the normal case with the servo components removed, in the supine examination state. (b) The PSD of the continuously acquired arterial pressure pulse for the normal case with the servo components removed in a 60° incline.

60° incline state is shown in Fig. 12(b). Note that the power spectra makes no obvious increases in both the LF and HF areas when the states changed from supine to incline for the NIDDM case.

The examples illustrated above demonstrate that the self-organizing arterial pressure pulse classification technique using ART2 has led to new insights in cardiovascular control. This

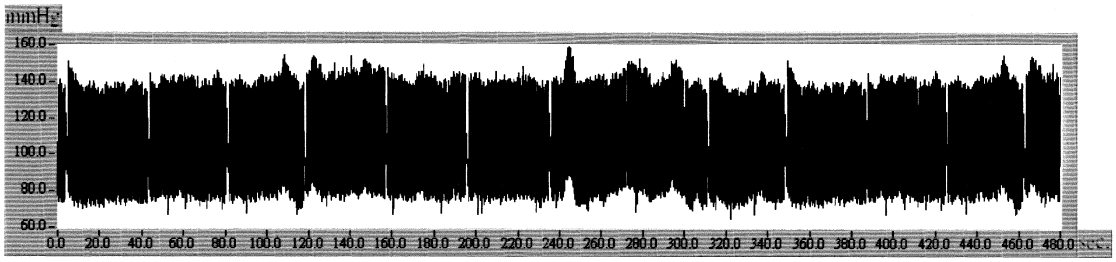

Fig. 9. An example of the acquired signal from Finapres after removing the servo components for the NIDDM patient.

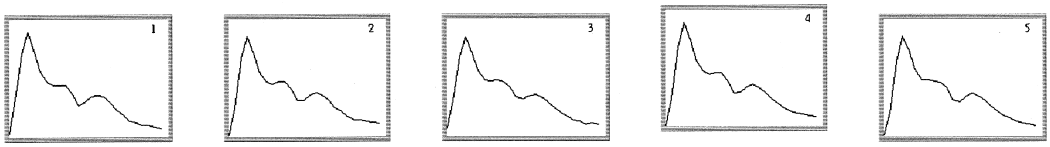

Fig. 10. The recognition categories of ART2 for the NIDDM patient shown in Fig. 9.

technology may also be used to study the involvement of the autonomic nervous system in the evolution of many diseased states. The technique provides at least three novel diagnostic tools for the clinical neurophysiology laboratory. First, the pieces affected by unexpected artificial motions (i.e. physical disturbance) can be determined easily by the ART2 network according to the status distribution plot. Therefore, clean segments corresponding to each clinical examination state can be obtained from the continuously acquired waveform. Second, a few categories will be created after applying the ART2 network to the input patterns (i.e. minimal cardiac cycles). The vigilance parameter of the ART2 network regulates the category coarseness of the input pattern. As the vigilance parameter becomes closer to 1.0, the system becomes more sensitive to the difference between the input pattern and the associated pattern. These pulse signal categories can then be useful to physicians for diagnosis in clinical application. Third, the status distribution plot provides an alternative method to assist physicians in evaluating the signs of abnormal and normal autonomic control. For instance, it is clear that there are more different categories around the moment of states when the monotoring position is changed from supine to incline for the normal case as shown in Fig. 7 than that of the ones for the NIDDM patient in Fig. 11. The possible reason is that this artificial motion performs more obviously for the normal case than in the NIDDM patient. Therefore, clinicians need not look at actual arterial pressure profiles after being trained to read the status distribution plots. The future work is to undertake a vigorous test of the specificity and sensitivity of diagnosis by the proposed method. Finally, it should be noted that generally group averages are used in the study of the PSD analysis being used to evaluate autonomic function in the context of diabetic neuropathy. The inherent variability of the PSD analysis makes application to a specific patient a hazardous approach. Therefore, the results of PSD analysis will not be used to change the course of a specific patient for the time being.

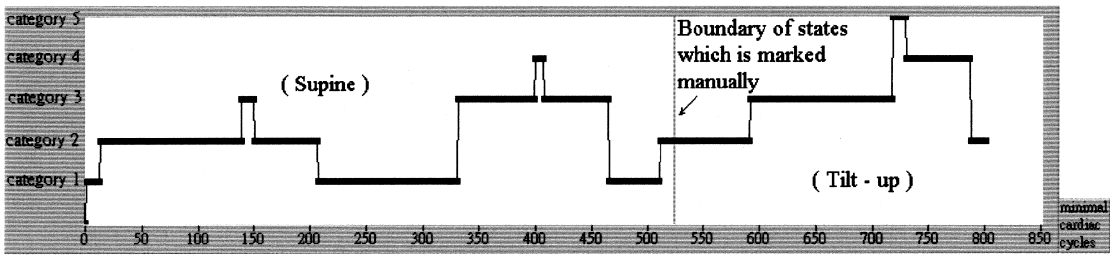

Fig. 11. Status distribution plot (SDP) for the NIDDM patient. Lateral axis is the continuous input numbers of minimal cardiac cycles. Straight axis: Category 1–5 denote five classified patterns.

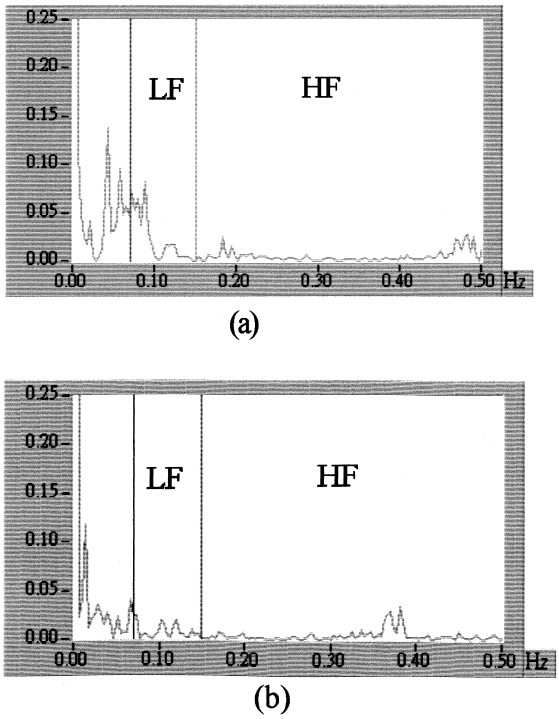

Fig. 12. (a) The PSD of the continuously acquired arterial pressure pulse from Finapre for the NIDDM patient with the removal of servo components at the supine examination state. (b) The PSD of the continuously acquired arterial pressure pulse for the NIDDM patient with the removal of servo components at the 60° incline.

4. Conclusions

A self-organizing classification system for the arterial pressure pulse based on the ART2 (adaptive resonance theory) network was developed. The technique provides at least three novel diagnostic tools in the clinical neurophysiology laboratory. First, the pieces affected by unexpected artificial motions (i.e. physical disturbance) can be determined easily by the ART2 network according to the status distribution plot. Second, a few categories will be created after applying the ART2 network to the input patterns (i.e. minimal cardiac cycles). These pulse signal categories can be useful to physicians for diagnosis in conventional clinical applications. Third, the status distribution plot provides an alternative method to assist physicians in evaluating the signs of abnormal and normal autonomic control. The proposed method has shown its clinical applicability for the examination of the autonomic nervous system.

Acknowledgements

This work is supported by National Science Council (NSC), Republic of China, under the grant numbers NSC-87-2213-E-035-033 and NSC-88-2815-C-035-031-E.

Appendix A

The potential, or STM activity, z_i of the ith node at any one of the F1 processing stages, i.e. s_i, x_i, v_i, u_i, p_i and q_i, obeys a membrane equation of the form:

$$\in \frac{\mathrm{d}}{\mathrm{d}t} z_i = -Az_i + (1 - Bz_i)J_i^+ - (C + Dz_i)J_i^- \tag{A.1}$$

($i = 1, \ldots, M$). J_i^+ is the total excitatory input to the ith node and J_i^- is total inhibitory input. In the absence of all inputs, z_i decays to 0. The dimensionless parameter $\in$ represents the ratio between the STM relaxation time and the LTM relaxation time.

$$0 < \in \ll 1 \tag{A.2}$$

Also, $\mathrm{B} \equiv 0$ and $\mathrm{C} \equiv 0$ in the F1 equation of the ART2. Thus the STM equations, in singular form as $\in \longrightarrow 0$, reduce to

$$V_i = \frac{J_i^+}{A + DJ_i^-} \tag{A.3}$$

In this form, the dimensionless Eqs. (A.4)– (A.10) characterize the STM activities, s_i, x_i, v_i, u_i, p_i and q_i, are computed at F1:

$$s_i = I_i + au_i \tag{A.4}$$

$$x_i = \frac{s_i}{e + \|S\|}; \quad e \text{ is a constant}, \quad 0 < e \ll 1 \tag{A.5}$$

$$p_i = u_i + \sum_{j=1}^{N} g(y_i)\hat{w}_{ji} \tag{A.6}$$

$$q_i = \frac{p_i}{e + \|P\|} \tag{A.7}$$

$$v_i = f(x_i) + bf(q_i) \tag{A.8}$$

$$u_i = \frac{v_i}{e + \|V\|} \tag{A.9}$$

$$\Delta u = \sum_{i=1}^{M} |u_i(k+1) - u_i(k)| \tag{A.10}$$

Where $S \equiv [s_1, s_2, \ldots, s_M]$, $V \equiv [v_1, v_2, \ldots, v_M]$ and $P \equiv [p_1, p_2, \ldots, p_M]$. $\|\cdot\|$ denotes the L_2-norm of a vector. y_j is the STM activity of the jth F2 node and w_{ji} is the LTM weight in the pathway from the jth F2 node to the ith F1 node. The nonlinear signal function $f(\cdot)$ in Eq. (A.11) is

chosen as follows.

$$f(x) = \begin{cases} \dfrac{2qx^2}{x^2+q^2}, & \text{if } 0 \le x < q \\ 0, & \text{if } x > q \end{cases} \tag{A.11}$$

which is continuously differentiable. Since the variables x_i and q_i are always between 0 and 1 (Eqs. (A.5) and (A.7)), the function values $f(x_i)$ and $f(q_i)$ also stay between 0 and 1. Alternatively, the signal function $f(x)$ is chosen to saturate at high x values. This causes the effect of flattening the pattern details.

The key properties of F2 are the contrast enhancement of filtered F1 → F2 input patterns and reset or enduring inhibition of active F2 nodes whenever a pattern is mismatched at F1, which is large enough to activate the orienting subsystem. Contrast enhancement is carried out by competition within F2. F2 makes a choice when the node receives the largest total input, which quenches activity in all other nodes. In other words, let T_j be the summed filtered F1 → F2 input to the jth F2 nodes:

$$T_i = \sum_{i=1}^{M} p_i w_{ij} \tag{A.12}$$

($j = \mathrm{M}+1, \ldots, \mathrm{N}$). Then F2 is said to make a choice if the Jth F2 node becomes maximally active, while all other nodes are inhibited, when

$$T_J = \max\{T_j : j = M+1 \ldots N\} \tag{A.13}$$

F2 reset may be carried out in several ways, one being the use of a gated dipole field network in F2. When a nonspecific arousal input reaches an F2 gated dipole field, nodes are inhibited or reset in proportion to their former STM activity levels. Moreover, this inhibition endures until the bottom-up input to F1 shuts off. Such a nonspecific arousal wave reaches F2, via the orienting subsystem, when a sufficiently large mismatch occurs at F1. When F2 makes a choice, the main element of the gated dipole field dynamics may be characterized as:

$$g(y_i) = \begin{cases} d, & \text{if the neuronin F2 receives largest input} \\ 0, & \text{otherwise} \end{cases} \tag{A.14}$$

The top-down and bottom-up LTM trace equations for ART2 are determined using

$$\text{Top-down (F2}\rightarrow\text{F1)}: \frac{\mathrm{d}}{\mathrm{d}t} w_{ji} = g(y_j)[p_i - w_{ji}] \tag{A.15}$$

$$\text{Bottom-up (F1}\rightarrow\text{F2)}: \frac{\mathrm{d}}{\mathrm{d}t} w_{ij} = g(y_j)[p_i - w_{ij}] \tag{A.16}$$

If F_2 makes a choice, (A.13)– (A.16) imply that, if the Jth F2 node is active, then

$$\frac{\mathrm{d}}{\mathrm{d}t} w_{Ji} = d[p_i - w_{Ji}] = d(1-d)\left[\frac{u_i}{1-d} - w_{Ji}\right] \tag{A.17}$$

and,

$$\frac{\mathrm{d}}{\mathrm{d}t}w_{Ji} = d[p_i - w_{Ji}] \tag{A.18}$$

with $0 < d < 1$. For all $j \neq J$, $(\mathrm{d}/\mathrm{d}t)w_{Ji} = 0$ and $(\mathrm{d}/\mathrm{d}t)w_{ij} = 0$.

In contrast, the computation of an analog pattern match does require pattern information. The degree of match between an STM pattern at F1 and an active LTM pattern is determined by the vector $R \equiv [r_1, r_2, \ldots, r_M]$, with

$$r_i = \frac{u_i(k) + cp_i(k)}{e + \|U(k)\| + \|cP(k)\|} \tag{A.19}$$

The orienting subsystem is assumed to reset F_2 whenever an input pattern is active and

$$(\|R\| = e) < \rho, \tag{A.20}$$

where the vigilance parameter ρ is set between 0 and 1.

References

[1] R. Schondorf, New investigation of autonomic nervous system function, Journal of Clinical Neurophysiology 10 (1993) 28–38.

[2] B.P.M. Imholz, et al., Non-invasive continuous finger blood pressure measurement during orthostatic stress compared to intra-arterial pressure, Cardiovascular Research 24 (1990) 214–221.

[3] G. Parati, et al., Comparison of finger and intra-arterial blood pressure monitoring at rest during laboratory resting, Hypertension 13 (1989) 647–655.

[4] B.P.M. Imholz, et al., Continuous finger arterial pressure: utility in the cardiovascular laboratory, Clinical Autonomic Research 1 (1991) 43–53.

[5] R.W. DeBoer, et al., Comparing spectra of a series of points events particularly for heart rate variability data, IEEE Transactions on Biomedical Engineering 31 (1984) 384–387.

[6] J.M. Karemaker, Analysis of blood pressure and heart rate variability: theoretical considerations and clinical applicability, Journal of Autonomic Nervous System 25 (1992) 315–329.

[7] T.r. Saul, et al., Transfer function analysis of the circulation: unique insights into cardiovascular regulation, American Journal of Physiology 261 (1991) 1231–1245.

[8] C.C. Chiu, S.J. Yeh, R.C. Lin, Data acquisition and validation analysis for Finapres signals, Chinese Journal of Medical and Biological Engineering 15 (1995) 47–58.

[9] S.J. Yeh, C.C. Chiu, Y.C. Yu, Autonomic Dysfunction of middle cerebral artery infarction, Biomedical Engineering, Applications, Basis and Communications 8 (1996) 40–45.

[10] G.A. Carpenter, S. Grossberg, in: Pattern recognition by self-organizing neural networks, MIT Press, Cambridge, MA, 1991, pp. 397–424.

[11] R.P. Lippmann, An introduction to computing with neural nets, IEEE Acoustics, Speech, Signal Processing Magazine 4 (1987) 4–22.

[12] D.R. Hush, B.G. Horne, Progress in supervised neural networks, IEEE Signal Processing Magazine 10 (1993) 8–39.

[13] W.J. Tompkins, in: Biomedical Digital Signal Processing, Prentice-Hall, Englewood Cliffs, NJ, 1993, pp. 55–77.

[14] J. Tepperman, in: Heart Rate Variability Physician's Guide, second ed., Marquette Electronics, 1995, pp. 1–35.

[15] B. Pomeranz, et al., Assessment of autonomic function in humans by heart rate spectral analysis, American Journal of Physiology 248 (1985) 151–153.

Chuang-Chien Chiu received a B.Sc. degree in Electrical Engineering from Feng Chia University, Taiwan, ROC in 1986. He received an M.Sc. degree in 1991 and a Ph.D. degree in 1993, both in Electrical Engineering, from Michigan State University, MI. Since 1993, he has been with the Department of Automatic Control Engineering, Feng Chia University, Taiwan, ROC, where he is currently an Associate Professor and Chairman. His current research interests include biomedical signal processing and neural networks, with particular emphasis on physiological signal analysis for autonomic nervous system, speech analysis, image processing and developing real-time medical system for tongue diagnosis and objective auscultation in traditional Chinese medical diagnosis.

Shoou-Jeng Yeh was born in Chia-Yi, Taiwan, in 1960. He received an MD degree from Taipei Medical College in 1987. Dr Yeh obtained his professional experience as a resident of neurology and internal medicine from 1988 till 1991. He has served as a neurologist and attending physician in the Section of Neurology and Department of Internal Medicine at Taichung Veterans General Hospital since 1992. Dr Yeh joined the Department of Neurology in Taichung Cheng-Ching Hospital in 1994 and, has been the Chief of Department of Neurology in the same hospital since 1995. His major research interests include non-invasive evaluation of autonomic disorders and he currently directs the autonomic and neurovascular unit, which consists of a room for thermal regulatory test and a room for autonomic reflex test.

Ching-Hsiu Chen was born in Tainan, Taiwan in 1978. He is currently working for a B.Sc. degree in the Department of Automatic Control Engineering at Feng Chia University, Taiwan, ROC. He has been an undergraduate research assistant in the Signal Processing and Biomedical System Laboratory at Feng Chia University since 1998.